

# Fast Inverse Compensation of Preisach-Type Hysteresis Operators Using Field-Programmable Gate Arrays

Xiaobo Tan and Omar Bennani

**Abstract**—Preisach-type operators model hysteresis via weighted superposition of a large (and even infinite) number of basic hysteretic elements (called hystérons), and they have proven capable of capturing various complicated hysteretic behaviors. While inverse compensation is an effective approach to control of hysteretic systems, inversion of Preisach-type operators is a bottleneck in demanding, high-speed applications due to the high computational cost. In this paper a novel and general framework is proposed for fast inversion of a wide class of Preisach-type operators, by exploiting the massive parallelism offered by field-programmable gate arrays (FPGAs) to process the inherently parallel hysteresis operators. The theory, algorithm, and implementation of the inversion are presented. The inversion output is computed iteratively with guaranteed convergence (up to machine precision) provided the hysteresis operator is piecewise monotone and Lipschitz continuous. For an operator consisting of  $m$  hystérons, the proposed approach shows a computational complexity of  $O(\log m)$ , in contrast to  $O(m)$  for methods using general DSPs. The effectiveness of the fast inversion approach is demonstrated by implementation results on open-loop tracking of kHz reference signals, based on inversion of a Krasnosel’skii-Pokrovskii operator.

## I. INTRODUCTION

Hysteresis is a nonlinear, nonlocal memory effect that can be found in diverse natural, social, and engineering systems. For instance, hysteresis presents itself in ferromagnetism and superconductivity [1], biology [2], economics [3], geosciences [4], and various smart materials [5]–[9]. Modeling, identification, and control of hysteresis nonlinearity has received much attention due to its sophisticated nature and wide implications in physical and engineering systems. An important class of hysteresis models are Preisach-type operators [1], [10], [11]. A Preisach-type operator is typically of phenomenological nature, and consists of a weighted superposition of a large (and even infinite) number of basic hysteretic elements (called *hystérons*). A few examples of Preisach-type operators include the classical Preisach operator, the Krasnosel’skii-Pokrovskii (KP) operator, the Prandtl-Ishlinskii (PI), and the homogenized energy model for hysteresis [9], [12] (which also carries physical interpretations). Preisach-type operators have proven effective in capturing complicated, hysteretic behaviors in a wide range of applications [1], [4]–[6], [8], [9], [13]–[15].

Control of hysteretic systems is challenging since traditional tools for systems with smooth dynamics do not apply directly. An effective approach to dealing with hysteresis nonlinearity is inverse compensation [16]–[18], where an

(approximate) inverse hysteresis operator is constructed to cancel the hysteretic effect. Hysteresis is often coupled with traditional linear or nonlinear dynamics. In that case, a feedback controller can be used jointly with the inverse hysteresis compensator to handle the remaining dynamics of the plant [6], [16], [17], [19]. This approach is illustrated in Fig. 1.

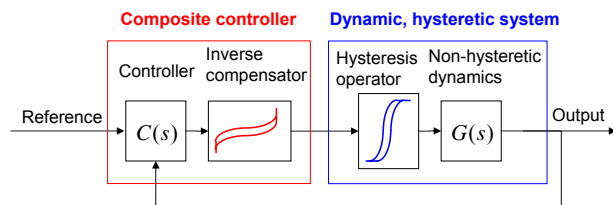


Fig. 1. A generic control approach combining feedback with inverse compensation of hysteresis (see, e.g., [16]).

The inversion problem for Preisach-type operators generally does not have analytical solutions. One exception is that the inverse of a play-type PI operator with a finite number of hystérons turns out to be a stop-type PI operator [18]. Another example is the pseudo-compensator concept [5], [20], where a Preisach operator is used to approximate the inverse of another Preisach operator (this is only exact for very special Preisach weighting functions [1]). In most cases, however, the inversion of a Preisach-type operator has to be carried out iteratively [14], [21]. All inverse operations, direct or iterative, involve evaluations of the outputs of all hystérons at each time step. When the operator has a large number of hystérons (a typical case in practice), the computational cost becomes prohibitive for general-purpose digital signal processors (DSPs), where the contributions of individual hystérons are evaluated sequentially. This presents a critical hurdle to the adoption of Preisach-type operators for hysteresis modeling and compensation in demanding, high-speed applications, e.g., ultrafast nanopositioning for data storage and for atomic force microscopy (AFM) imaging.

In this paper a unified approach to fast inversion of a broad class of Preisach-type operators is presented by exploiting the massive parallelism offered by field-programmable gate arrays (FPGAs). An FPGA is used as an embedded compensator to cancel (approximately) the hysteresis, and its parallel nature makes it particularly suitable for processing the inherently parallel Preisach-type operators. We discuss the theory, algorithm, and implementation of the embedded inversion approach. The inversion output is computed using a fixed-point iteration algorithm, with guaranteed convergence

X. Tan and O. Bennani are with the Smart Microsystems Laboratory, Department of Electrical and Computer Engineering, Michigan State University, East Lansing, MI 48824, USA. {xibtan, benannio}@egr.msu.edu

(up to machine precision) provided the hysteresis operator is piecewise monotone and Lipschitz continuous. For a given tolerance, the algorithm completes in a finite number of iterations. For an operator consisting of  $m$  hysterons, we show that the proposed approach requires only a computational complexity of  $O(\log m)$ , in contrast to  $O(m)$  for methods using general DSPs. The effectiveness of the fast inversion approach is demonstrated by implementation results on open-loop tracking of kHz reference signals, based on inversion of a Krasnosel'skii-Pokrovskii operator.

It should be noted that there has been some past work on embedded hysteresis inversion. Davino and coworkers [22], [23] developed an efficient inversion algorithm for the classical Preisach operator by storing the samples of Everett function in a lookup table and then using interpolations, and they demonstrated the implementation in a microcontroller. Janocha et al. implemented the inversion of a PI operator in FPGA [24]. Comparing to these past studies, our approach has two salient features: 1) it is applicable to a general class of Preisach-type operators and not restricted to just one specific operator, and 2) it is amenable to incorporation of embedded adaptation, which is particularly important for smart material-actuated systems since the hysteretic behaviors are often sensitive to environmental conditions.

The remainder of the paper is organized as follows. In Section II Preisach-type operators are reviewed, and their properties relevant to the inversion algorithm are studied. The inversion framework is described in Section III. Implementation of the embedded FPGA compensator is presented in Section IV. Finally, concluding remarks are provided in Section V.

## II. PREISACH-TYPE OPERATORS

### A. Definition of Preisach-Type Operators

A Preisach-type operator models hysteresis through weighted superposition of possibly a continuum of basic hysteretic elements, called hysterons. One example of Preisach-type operators is the Krasnosel'skii-Pokrovskii (KP) operator, which is illustrated in Fig. 2. We will describe KP operators and their relevant properties first, and then have a brief discussion on other Preisach-type operators. Consider a KP hysteron depicted in Fig. 2(a), which is characterized by a pair of thresholds  $(\beta, \alpha)$ . Define a ridge function  $\delta: \mathbb{R}^+ \rightarrow [-1, 1]$ :

$$\delta(x) = \begin{cases} -1 & \text{if } x < 0 \\ -1 + \frac{2x}{a} & \text{if } 0 \leq x \leq a \\ 1 & \text{if } x > a \end{cases}, \quad (1)$$

where  $a$  is the distance shown in Fig. 2(a). Let  $C([0, T])$  denote the space of continuous functions on  $[0, T]$ . Given an input  $v(\cdot) \in C([0, T])$  and an initial output value  $\zeta \in [-1, 1]$ , the output of the hysteron  $w = \gamma_{\beta, \alpha}[v(\cdot), \zeta] \in C([0, T])$  is defined as follows:

$$w(t) = \begin{cases} \max\{w(t^-), \delta(v(t) - \alpha)\} & \text{if } v(t) > v(t^-) \\ \min\{w(t^-), \delta(v(t) - \beta)\} & \text{if } v(t) < v(t^-) \\ w(t^-) & \text{if } v(t) = v(t^-) \end{cases}, \quad (2)$$

where  $w(0^-) = \zeta$ ,  $t^- = \lim_{\varepsilon \downarrow 0} t - \varepsilon$ .

A KP operator  $\Gamma$  is a weighted combination of  $m$  KP hysterons with different threshold pairs,  $(\beta_i, \alpha_i)$ ,  $i = 1, \dots, m$ , as illustrated in Fig. 2(b). Note that all hysterons share the same ridge function  $\delta$ , characterized by the parameter  $a$ . Each hysteron has a weight  $\mu(\beta_i, \alpha_i)$ , which is typically assumed to be nonnegative. Given an input  $v(\cdot) \in C([0, T])$  and the initial condition  $\{\zeta_i\}_{i=1}^m$ , the output  $u = \Gamma[v(\cdot), \{\zeta_i\}]$  reads:

$$u(t) = \sum_{i=1}^m \mu(\beta_i, \alpha_i) \gamma_{\beta_i, \alpha_i}[v(\cdot), \zeta_i](t). \quad (3)$$

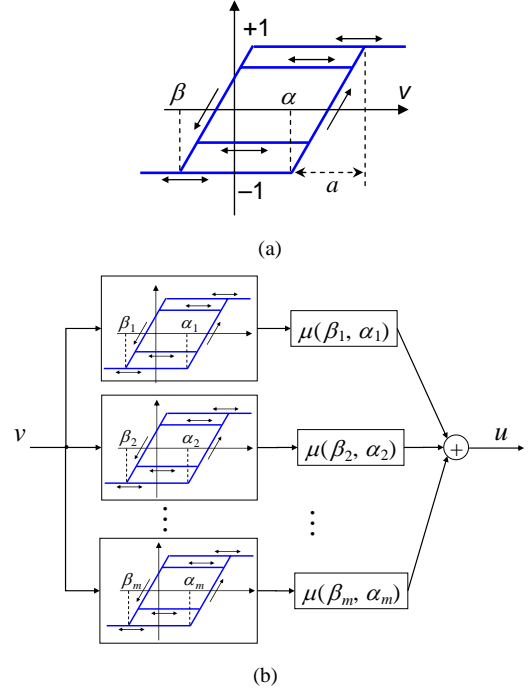


Fig. 2. (a) A KP hysteron  $\gamma_{\beta, \alpha}$ ; (b) Illustration of the KP operator.

More generally, one can define a KP operator consisting of a continuum of hysterons. Define the half plane  $\mathcal{P} = \{(\beta, \alpha) : \beta \leq \alpha\}$ . Given a Borel measurable configuration of all hysterons,  $\zeta_0: \mathcal{P} \rightarrow [-1, 1]$ , the output  $u$  of the KP operator can be expressed as

$$u(t) = \Gamma[v(\cdot), \zeta_0](t) = \int_{\mathcal{P}} \mu(\beta, \alpha) \gamma_{\beta, \alpha}[v(\cdot), \zeta_0(\beta, \alpha)](t) d\beta d\alpha, \quad (4)$$

where  $\mu$  is a Borel measurable density function that is integrable on  $\mathcal{P}$ . One can assume that  $\mu$  has a compact support, in which case it suffices to consider a compact subset  $\mathcal{P}_0 \subset \mathcal{P}$ :

$$\mathcal{P}_0 = \{(\beta, \alpha) : -r_0 \leq \beta \leq \alpha \leq r_0, \},$$

for some  $r_0 > 0$ .

Using variants of the KP hysteron as building elements, one can obtain other Preisach-type operators. For instance, the classical Preisach operator uses the delayed relays as hysterons (Fig. 3(a)), which are also characterized by a

pair of thresholds  $(\beta, \alpha)$ . Weighted superposition of linear play operators (Fig. 3(b)) and that of linear stop operators (Fig. 3(c)), lead to the Prandtl-Ishlinskii (PI) operators of the play type, and of the stop type, respectively. Note that play or stop operators are parameterized by a single variable  $r$  instead of a pair.

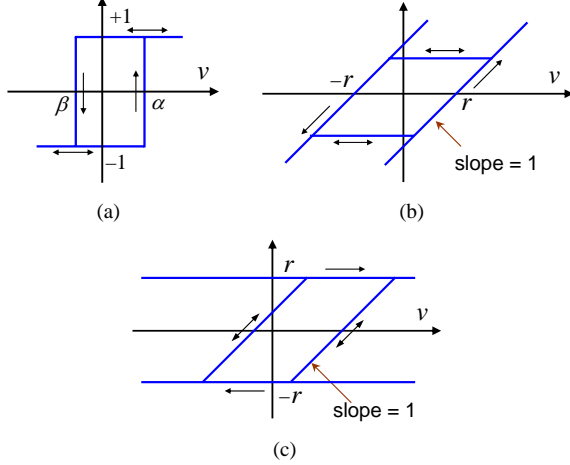


Fig. 3. (a) A Preisach hysteron; (b) a play operator; (c) a stop operator.

### B. Properties of Preisach-Type Operators

The inversion algorithm to be presented requires two properties of Preisach-type operators, *piecewise monotonicity* and *Lipschitz continuity*, which are precisely defined below.

**Definition 2.1:** A Preisach-type operator  $\Gamma$  is *piecewise monotone* if, given a monotone input  $v \in C([0, T])$  for arbitrary  $T > 0$  and any initial condition  $\zeta_0$ , the following holds:

$$(\Gamma[v(\cdot), \zeta_0](T) - \Gamma[v(\cdot), \zeta_0](0)) \cdot (v(T) - v(0)) \geq 0. \quad (5)$$

**Definition 2.2:** A Preisach-type operator  $\Gamma$  is *Lipschitz continuous* if, given a monotone input  $v \in C([0, T])$  for arbitrary  $T > 0$  and any initial condition  $\zeta_0$ , for any  $t_1, t_2 \in [0, T]$ , the following holds:

$$|\Gamma[v(\cdot), \zeta_0](t_2) - \Gamma[v(\cdot), \zeta_0](t_1)| \leq L|v(t_2) - v(t_1)|, \quad (6)$$

for some constant  $L > 0$ .

Note that an alternative definition of Lipschitz continuity can be given using the  $L_\infty$  norm of  $C([0, T])$  [25]. Definition 2.2, however, suffices for the purpose of this paper.

**Proposition 2.1:** Let the weighting function  $\mu$  be non-negative. Then all the Preisach-type operators described in Section II-A (i.e., the KP operator, the classical Preisach operator, and the PI operators of play/stop types) are piecewise monotone.

*Proof.* It is clear that each hysteron satisfies (5) if one replaces  $\Gamma$  by a hysteron  $\gamma$ . The claim then follows considering the definition of a Preisach-type operator and the nonnegativity assumption on the weighting function  $\mu$ .  $\square$

We next establish the Lipschitz continuity of the KP operator under fairly general conditions.

**Proposition 2.2:** A KP operator is Lipschitz continuous if

- 1) it consists of a finite number of hysterons (see (3)); or
- 2) it consists of a continuum of hysterons (see (4)), where the weighting function  $\mu$  is Borel measurable and integrable on  $\mathcal{P}$ .

*Proof.* First consider the case 1). Suppose that the input increases from  $v$  to  $v + \Delta v$  for sufficiently small  $\Delta v > 0$ . A necessary condition for the output of a hysteron  $\gamma_{\beta_i, \alpha_i}$  to increase is  $v \in [\alpha_i, \alpha_i + a)$ . Define the set of hysterons  $S^+(v)$  as

$$S^+(v) \triangleq \{i : v - a < \alpha_i \leq v\}.$$

The output increase for a hysteron in  $S^+(v)$  is at most  $\frac{2\Delta v}{a}$ , and thus the output increase for the KP operator under an input increase of  $\Delta v$  is bounded by  $L^+\Delta v$ , where

$$L^+ \triangleq \sup_v \sum_{i \in S^+(v)} \frac{2|\mu(\beta_i, \alpha_i)|}{a}. \quad (7)$$

Similarly, one can show that the output decrease for the KP operator corresponding to an input decrease of  $\Delta v$  is bounded by  $L^-\Delta v$ , with

$$L^- \triangleq \sup_v \sum_{i \in S^-(v)} \frac{2|\mu(\beta_i, \alpha_i)|}{a}, \quad (8)$$

$$S^-(v) \triangleq \{i : v - a \leq \beta_i < v\}.$$

Note that  $L = \max\{L^+, L^-\}$  is bounded since the total number of hysterons is finite. It is clear that the KP operator (3) is Lipschitz with constant  $L$ .

The proof for case 2) is analogous and its details will be omitted. The Lipschitz constant  $L$  in this case is

$$\begin{aligned} L &= \max\{L^+, L^-\}, \\ L^+ &\triangleq \sup_v \frac{2}{a} \int_{v-a}^v \int_{-\infty}^{\alpha} |\mu(\beta, \alpha)| d\beta d\alpha, \\ L^- &\triangleq \sup_v \frac{2}{a} \int_{v-a}^v \int_{\beta}^{\infty} |\mu(\beta, \alpha)| d\alpha d\beta. \end{aligned}$$

The boundedness of  $L$  follows from the integrability of  $\mu$ .  $\square$

**Remark 2.1:** One can also show the Lipschitz continuity of a KP operator that has a mixture of discrete and continuum hysterons. Proposition 2.2 can be easily extended to PI operators, thanks to the finite slopes of their hysterons. However, for classical Preisach operators, the Lipschitz continuity only holds for the continuum case (with appropriate condition on  $\mu$ ). For a Preisach operator consisting of countable hysterons, its output takes values in a countable set. The consequence of this discontinuity in hysteresis inversion will be discussed in Section III.

### III. INVERSION ALGORITHM

Fig. 4 illustrates the idea of hysteresis inversion. Given a desired output trajectory  $u_d(\cdot)$  and an initial condition  $\zeta_0$  for a Preisach-type operator  $\Gamma$ , the (approximate) inverse operator  $\hat{\Gamma}^{-1}$  generates  $v(\cdot)$  as the input to  $\Gamma$ , such that  $u(t) = \Gamma[v(\cdot), \zeta_0](t) \approx u_d(t)$ , i.e.,  $\Gamma \circ \hat{\Gamma}^{-1} \approx \text{Identity operator}$ .  $\hat{\Gamma}^{-1}$  defined this way is called the *right* (as opposed to *left*)

inverse of  $\Gamma$ , which is typically used for cancellation of hysteresis preceding other dynamics. A feedback controller can then be designed to handle the remaining non-hysteretic dynamics (see Fig. 1).

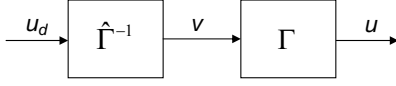


Fig. 4. Illustration of hysteresis inversion.

In the interest of digital control, the inversion algorithm will be discussed in discrete time. The initial condition  $\zeta(0)$  of the Preisach-type operator is assumed to be known. In practice, this can be achieved by applying certain (e.g., maximum or minimum) initialization input [6]. The initial condition, together with the past input history  $v(\cdot)$ , allows one to keep track of the states of hysterons at any time instant  $n$ . Given the current configuration of hysterons  $\zeta(n)$ , the inversion problem is to find the input value  $v(n+1)$  so that the hysteresis output is equal (or close) to the desired value  $u_d(n+1)$  for the next time instant  $n+1$ . It is implicitly understood that the input changes monotonically from  $v(n)$  to  $v(n+1)$  to avoid any ambiguity in evaluating the hysteresis operator.

The following two assumptions are made about  $\Gamma$ :

- **(A1)**  $\Gamma$  is piecewise monotone;
- **(A2)**  $\Gamma$  is Lipschitz continuous with constant  $L > 0$ .

The inversion algorithm computes the value for  $v(n+1)$  iteratively:

$$\begin{cases} v^{[k+1]}(n+1) = v^{[k]}(n+1) + \frac{u_d(n+1) - \Gamma[v^{[k]}(n+1), \zeta(n)]}{L} \\ v^{[0]}(n+1) = v(n) \end{cases} \quad (9)$$

The algorithm (9) was adapted from the inversion algorithm for a classical Preisach operator in the space of piecewise monotone, continuous functions [21].

*Proposition 3.1:* Suppose that the input is restricted to  $[v_{min}, v_{max}]$ . Let  $u_{sat}^-$  and  $u_{sat}^+$  denote the negative and positive saturation values of  $\Gamma$ , respectively. Let **(A1)** and **(A2)** be valid. Then for any  $u_d(n+1) \in [u_{sat}^-, u_{sat}^+]$ , the algorithm (9) converges,  $v^{[k]}(n+1) \rightarrow v^*(n+1)$  as  $k \rightarrow \infty$ , where  $v^*(n+1)$  satisfies  $\Gamma[v^*(n+1), \zeta(n)] = u_d(n+1)$ . Furthermore, given any  $\varepsilon > 0$ , the following holds:

$$\left| \Gamma[v^{[k]}(n+1), \zeta(n)] - u_d(n+1) \right| \leq \varepsilon, \quad (10)$$

for  $k \geq N_\varepsilon$ , where  $N_\varepsilon$  is the smallest integer satisfying  $N_\varepsilon \geq L(v_{max} - v_{min})/\varepsilon$ .

*Proof.* Without loss of generality, assume  $u_d(n+1) > \Gamma[v(n), \zeta(n)]$ . With induction, one can show that  $\{v^{[k]}(n+1)\}_k$  is a strictly increasing sequence using **(A1)** and **(A2)**. The sequence is upper bounded by  $v_{max}$ , hence  $\lim_{k \rightarrow \infty} v^{[k]}(n+1)$  exists. Denote the limit by  $v^*(n+1)$ . The (Lipschitz) continuity of  $\Gamma$  implies

$$\Gamma[v^{[k]}(n+1), \zeta(n)] \rightarrow \Gamma[v^*(n+1), \zeta(n)],$$

as  $k \rightarrow \infty$ . From (9),

$$v^*(n+1) = v^*(n+1) + \frac{u_d(n+1) - \Gamma[v^*(n+1), \zeta(n)]}{L},$$

implying  $\Gamma[v^*(n+1), \zeta(n)] = u_d(n+1)$ .

When  $\left| \Gamma[v^{[k]}(n+1), \zeta(n)] - u_d(n+1) \right| > \varepsilon$ , the increment during each iteration is larger than  $\frac{\varepsilon}{L}$ . Since the range of the input is limited to  $[v_{min}, v_{max}]$ , the last statement of the proposition has to hold.  $\square$

The proposition provides an upper bound on the number of iterations for the inversion error to reach any tolerance (above the machine precision). In the context of FPGA-based embedded inversion, Preisach-type operators consisting of a finite number of hysterons are of practical interest. From the discussions in Section II-B, the algorithm (9) is then directly applicable to KP and PI operators. For classical Preisach operators (with discrete hysterons), however, there is a limit on how small the tolerance  $\varepsilon$  can be chosen. An alternative (approximate) inversion algorithm for such Preisach operators is the *closest-match* algorithm proposed by Tan and coworkers [26], which requires only the property of piecewise monotonicity.

#### IV. FPGA IMPLEMENTATION OF INVERSE HYSTERESIS COMPENSATOR

An FPGA is a silicon device containing high-density programmable logic components and interconnects, which can be reconfigured by an end user (hence the term “field-programmable”) to perform fast application-specific processing [27]. The speed and the processing power of FPGAs are comparable to those of application-specific integrated circuit (ASIC) chips, but they offer several important advantages over ASICs, e.g., instant manufacturing turnaround, low start-up costs, and ease of design changes.

Each iteration of the inversion algorithm (9) involves the evaluation of the Preisach-type operator  $\Gamma$ . When the operator has a large number of hysterons (a typical case in practice), the computational cost becomes prohibitive for general-purpose digital signal processors (DSPs), where the contributions of individual hysterons are evaluated sequentially. The parallel computing paradigm of FPGAs, however, is especially suitable for Preisach-type operators - such an operator is parallel in nature since all hysterons receive the same input. In addition, the characteristics of a hysteron can often be best described using logic elements, leading to convenient implementation of hysterons on FPGAs.

Fig. 5 shows the diagram for implementing the hysteresis inversion algorithm on FPGA. While the KP operator is used as an example, the general structure applies to PI operators and other Preisach operators meeting conditions **(A1)** and **(A2)**.

Note that although the evaluations of all hysterons can be performed in parallel, the summation on weighted hysteron outputs is a bottleneck. To minimize the computation time, an adder tree is implemented for the summation. For example, suppose that the number of hysterons  $m = 8$ . The first level of the adder tree will have four adders, each adding the

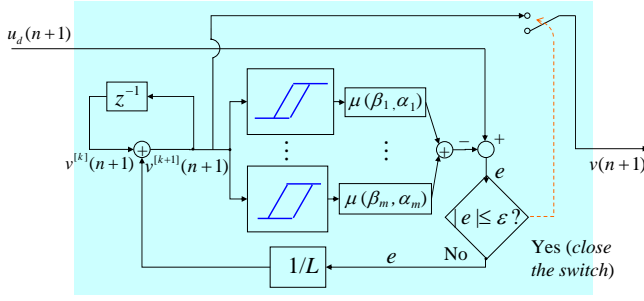


Fig. 5. Implementation of the hysteresis inversion algorithm in FPGA.

contributions from a pair of hysterons. The second level will have two adders, each adding the results of a pair of adders from the previous level. The third and last level will have just one adder, adding the results of the adders from the second level. Therefore a total of three clock cycles is needed for completing the summation operation. In general, the adder tree for  $m$  hysterons will take  $\log_2 m$  clock cycles. Since the summation is the speed-limiting factor in the FPGA-based hysteresis inversion, the computational time scales as  $O(\log_2 m)$  with respect to the number of hysterons  $m$ . This is in contrast to the  $O(m)$  time-complexity required by general-purpose DSPs. One can further speed up the inversion process in FPGA by implementing pipelining for the summation process.

As an example, the inversion algorithm (9) has been implemented on a Xilinx Virtex-II Pro FPGA. The implementation utilizes only logic resources, and deliberately avoids using the two on-chip PowerPC cores and RAM resources, which may not be available for low-end FPGAs. The implementation for inverting a KP operator with 21 hysterons takes about 30% of the logic resources on Virtex-II Pro. The device usage can be further reduced through optimization of resource allocation. Each iteration (9) in the inversion takes 11 clock cycles to complete. This implies close to  $5 \times 10^6$  iterations per second if a 50 MHz clock is used.

The thresholds of hysterons are chosen based on a regular lattice on the  $(\beta, \alpha)$  plane, as illustrated in Fig. 6. The evaluation of a KP hysteron (2) involves the shifted ridge function of the form  $\delta(v(t) - c)$ , with  $c = \beta_i$  or  $\alpha_i$ . To save multiplier resources, the slope portion of (1) is rewritten as

$$-1 + \frac{2(v(t) - c)}{a} = v(t) \cdot \frac{2}{a} - \frac{a + 2c}{a}.$$

For every new input  $v(t)$ , the product  $v(t) \cdot \frac{2}{a}$  is evaluated only once, and then each hysteron accesses the product and shifts it by  $-\frac{a+2c}{a}$  (pre-computed and stored) with the corresponding  $c$ .

Experiments have been conducted to verify the FPGA-based inversion algorithm. A collection of weights is assigned to the 21 KP hysterons. The values of the weights are shown in Fig. 7. An example of the hysteresis loop for this KP operator is shown in Fig. 8. The range of the input and the output of FPGA is set to be  $[-10, 10]$  V through

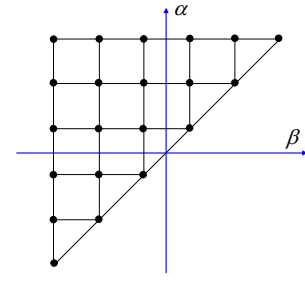


Fig. 6. Threshold pairs (represented by black dots) for the KP operator.

A/D and D/A interfaces.

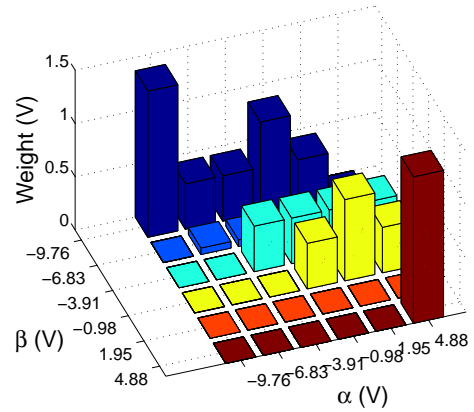


Fig. 7. Hysteron weights used for verification of inversion.

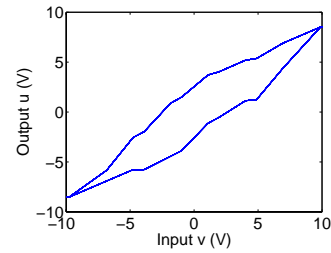


Fig. 8. Hysteresis loop of the KP operator with weights in Fig. 7.

A reference trajectory  $u_d(\cdot)$ , generated from a PC (through dSPACE DS1104), is sent to the FPGA hysteresis compensator. The inversion output  $v(\cdot)$  is then converted to an analog signal and acquired by dSPACE. The “achieved” output  $u(\cdot)$  of the KP operator is evaluated in Matlab based on the input  $v(\cdot)$ , and compared to the reference  $u_d(\cdot)$ . Fig. 9 shows the comparison between  $u_d$  and  $u$  when  $u_d$  is a sinusoidal signal with frequency 1000 Hz, while Fig. 10 shows the result when  $u_d$  is a combination of two sinusoids (300 Hz and 50 Hz). In both experiments, the tracking performance is satisfactory, where the tracking error is consistent with the set tolerance  $\varepsilon = 0.1$  in inversion.

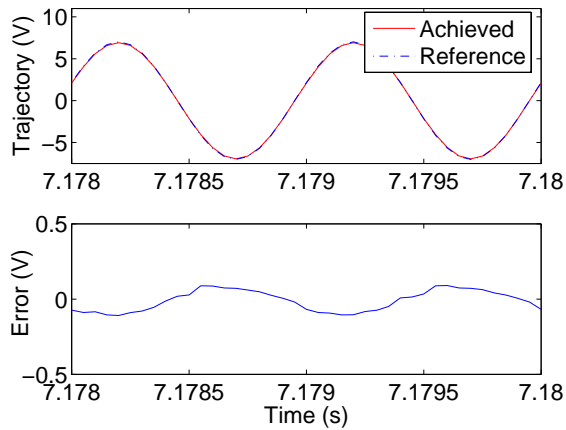


Fig. 9. Embedded inversion-based tracking performance for a 1 kHz reference signal.

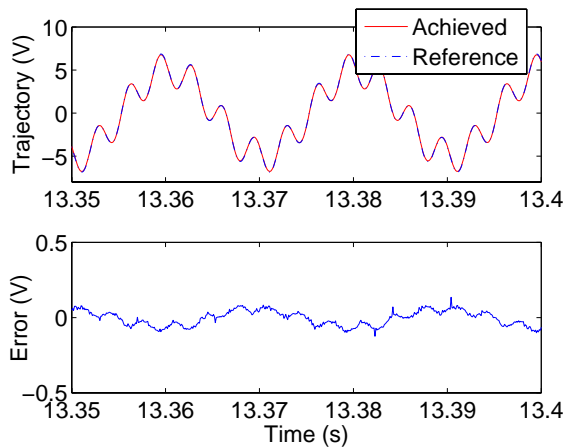


Fig. 10. Embedded inversion-based tracking performance for a reference signal consisting of 300 Hz and 50 Hz components.

## V. CONCLUSIONS

In this paper a unified, embedded approach to hysteresis compensation was presented for Preisach-type operators. The approach exploits the massive parallelism available in FPGAs to speed up the otherwise time-consuming inversion process. The reprogrammable nature of FPGAs allows one to find the most appropriate Preisach-type operators for specific applications without changing the architecture of the compensator. Implementation results were reported on inversion of a KP operator. One potential application of this work is to use the embedded hysteresis compensator as a plug-on device for smart material actuators, such as piezoelectric or magnetostrictive actuators. By eliminating the bottleneck in control of such hysteretic systems, one can realize precision tracking control with very high bandwidth (over kHz).

Future work includes incorporating parameter adaptation [28] into the hysteresis inversion framework. The parallel processing capability of FPGA will again be advantageous in that it allows hysteron weights to be updated simultaneously.

The embedded compensator will also be combined with feedback control and applied to demanding applications such as high-speed nanopositioning driven by (hysteretic) piezoelectric actuators.

## ACKNOWLEDGMENT

This work was supported in part by the MSU Quality Funds on High Assurance Systems.

## REFERENCES

- [1] I. D. Mayergoyz, *Mathematical Models of Hysteresis and Their Applications*. New York, NY: Elsevier, 2003.
- [2] D. Angeli, J. E. Ferrell, Jr., and E. D. Sontag, "Detection of multistability, bifurcations, and hysteresis in a large class of biological positive-feedback systems," *Proceedings of the National Academy of Sciences*, vol. 101, pp. 1822–1827, 2004.
- [3] A. Dixit, "Hysteresis, import penetration, and exchange rate pass-through," *The Quarterly Journal of Economics*, vol. 14, no. 2, pp. 205–228, 1989.
- [4] R. A. Guyer, K. R. McCall, and G. N. Boitnott, "Hysteresis, discrete memory and nonlinear wave propagation in rock," *Physical Review Letters*, vol. 74, pp. 3491–3494, 1994.
- [5] D. Croft, G. Shed, and S. Devasia, "Creep, hysteresis, and vibration compensation for piezoactuators: Atomic force microscopy application," *Journal of Dynamic Systems, Measurement, and Control*, vol. 123, no. 1, pp. 35–43, 2001.
- [6] X. Tan and J. S. Baras, "Modeling and control of hysteresis in magnetostrictive actuators," *Automatica*, vol. 40, no. 9, pp. 1469–1480, 2004.
- [7] R. V. Iyer and M. Shirley, "Hysteresis parameter identification with limited experimental data," *IEEE Transactions on Magnetics*, vol. 40, no. 5, pp. 3227–3239, 2004.
- [8] Z. Chen, X. Tan, and M. Shahinpoor, "Quasi-static positioning of ionic polymer-metal composite (IPMC) actuators," in *Proceedings of IEEE/ASME International Conference on Advanced Intelligent Mechatronics*, Monterey, CA, 2005, pp. 60–65.
- [9] R. Smith, *Smart Material Systems: Model Development*. Philadelphia, PA: SIAM, 2005.
- [10] M. A. Krasnosel'skii and A. V. Pokrovskii, *Systems with Hysteresis*. Springer Verlag, 1989.
- [11] M. Brokate and J. Sprekels, *Hysteresis and Phase Transitions*. New York: Springer-Verlag, 1996.
- [12] R. C. Smith, S. Seelecke, Z. Ounaies, and J. Smith, "A free energy model for hysteresis in ferroelectric materials," *Journal of Intelligent Material Systems and Structures*, vol. 14, no. 11, pp. 719–739, 2003.
- [13] H. T. Banks, A. J. Kurdila, and G. Webb, "Identification of hysteretic control influence operators representing smart actuators, Part I: Formulation," *Mathematical Problems in Engineering*, vol. 3, no. 4, pp. 287–328, 1997.
- [14] K. K. Leang and S. Devasia, "Iterative feedforward compensation of hysteresis in piezo positioners," in *Proceedings of the 42nd IEEE Conference on Decision and Control*, Maui, Hawaii, 2003, pp. 2626–2631.
- [15] J. Ahrens, X. Tan, and H. K. Khalil, "Multirate sampled-data output feedback control of smart material actuated systems," in *Proceedings of the American Control Conference*, New York, NY, 2007, to appear.
- [16] G. Tao and P. V. Kokotovic, "Adaptive control of plants with unknown hysteresis," *IEEE Transactions on Automatic Control*, vol. 40, no. 2, pp. 200–212, 1995.
- [17] —, *Adaptive Control of Systems with Actuator and Sensor Nonlinearities*. New York: John Wiley & Sons, Inc., 1996.
- [18] K. Kuhnen, "Modeling, identification and compensation of complex hysteretic nonlinearities - a modified prandtl-ishlinskii approach," *European Journal of Control*, vol. 9, no. 4, pp. 407–418, 2003.
- [19] X. Tan and H. K. Khalil, "Control of unknown dynamic hysteretic systems using slow adaptation: Preliminary results," in *Proceedings of the American Control Conference*, New York, NY, 2007, pp. 3294–3299.
- [20] C. Natale, F. Velardi, and C. Visone, "Identification and compensation of Preisach hysteresis models for magnetostrictive actuators," *Physica B*, vol. 2001, pp. 161–165, 2001.

- [21] R. V. Iyer, X. Tan, and P. S. Krishnaprasad, "Approximate inversion of the Preisach hysteresis operator with application to control of smart actuators," *IEEE Transactions on Automatic Control*, vol. 50, no. 6, pp. 798–810, 2005.
- [22] D. Davino, C. Natale, S. Pirozzi, and C. Visone, "A fast compensation algorithm for real-time control of magnetostrictive actuators," *Journal of Magnetism and Magnetic Materials*, vol. 290-291, pp. 1351–1354, 2005.
- [23] D. Davino, A. Giustiniani, V. Vacca, and C. Visone, "Embedded hysteresis compensation and control on a magnetostrictive actuator," *IEEE Transactions on Magnetics*, vol. 42, no. 10, pp. 3443–3445, 2006.
- [24] H. Janocha, D. Pesotski, and K. Kuhnen, "FPGA-based compensator of hysteretic actuator nonlinearities for highly dynamic applications," in *Proceedings of the 10th International Conference on New Actuators*, 2006, pp. 1013–1016.
- [25] A. Visintin, *Differential Models of Hysteresis*. Berlin: Springer, 1994.
- [26] X. Tan, R. Venkataraman, and P. S. Krishnaprasad, "Control of hysteresis: Theory and experimental results," in *Modeling, Signal Processing, and Control in Smart Structures*, ser. Proceedings of SPIE, V. Rao, Ed., vol. 4326. Bellingham, WA: SPIE, 2001, pp. 101–112.
- [27] S. Brown and J. Rose, "FPGA and CPLD architectures: A tutorial," *IEEE Design and Test of Computers*, vol. 13, no. 2, pp. 42–57, 1996.
- [28] X. Tan and J. S. Baras, "Adaptive identification and control of hysteresis in smart materials," *IEEE Transactions on Automatic Control*, vol. 50, no. 6, pp. 827–839, 2005.